Available online at www.sciencedirect.com
SCIENCE DIRECT®
Journal of Pharmaceutical and Biomedical Analysis
35 (2004) 75–86
JOURNAL OF PHARMACEUTICAL AND BIOMEDICAL ANALYSIS
www.elsevier.com/locate/jpba

Physicochemical characterization and dissolution properties of meloxicam–cyclodextrin binary systems☆

N. Buchi Naidu[a,b,*], K.P.R. Chowdary[a], K.V.R. Murthy[a], V. Satyanarayana[b], A.R. Hayman[c], G. Becket[d]

[a] *Department of Pharmaceutical Sciences, Andhra University, Visakhapatnam, India*
[b] *Division of Pharmaceutical Sciences, College of Pharmacy, University of Kentucky, Rose street, Lexington, KY, USA*
[c] *Department of Chemistry, University of Otago, Dunedin, New Zealand*
[d] *School of Pharmacy, University of Otago, Dunedin, New Zealand*

Received 4 December 2003; received in revised form 5 January 2004; accepted 7 January 2004

Abstract

The objective of the work is physicochemical characterization of meloxicam (ME)–cyclodextrin (CD) binary systems both in solution and solid states and to improve the dissolution properties of meloxicam via complexation with α-, β- and γ-cyclodextrins. Detection of inclusion complexation was done in solution state by means of phase solubility analysis, mass spectrometry and ^{1}H nuclear magnetic resonance (NMR) studies, and in solid state using differential scanning calorimetry (DSC), powder X-ray diffractometry, and in vitro dissolution studies. Phase solubility, mass spectrometry and ^{1}H NMR studies in solution state revealed 1:1 M complexation of meloxicam with all CDs. A true inclusion of ME with γ-CD at 1:1 and 1:2 M in solid state was confirmed by DSC, powder XRD and scanning electron microscopy (SEM) studies. Dissolution properties of ME–CDs binary systems were superior when compared to pure ME.

Keywords: Meloxicam; Cyclodextrins; Physicochemical characterization; Dissolution properties

1. Introduction

Meloxicam (ME) (4-hydroxy–2–methyl-*N*-(5-methyl-2-thiazolyl)-2H benzothiazine-3-carboxamide-1, 1-dioxide) is a highly potent non-steroidal anti-inflammatory drug (NSAID) of the enolic acid class of oxicam derivatives. The structure of meloxicam is shown in Fig. 1. It is used to treat rheumatoid arthritis, osteoarthritis, and other joint diseases. Meloxicam is a potent inhibitor of cyclooxygenase (COX) [1] and in several models shows selectivity for the inducible COX-2 isoenzyme [2–4]. This may explain the effectiveness and superior safety profile of this drug [5] since the therapeutic benefits are combined with good gastro-intestinal tolerability [6]. Like many NSAIDs, meloxicam is practically insoluble in water. The poor aqueous solubility and wettability of meloxicam leads to difficulties in formulating oral and parenteral

☆ Supplementary data associated with this article can be found at doi: 10.1016/j.jpba.2004.01.003.

* Corresponding author. Tel.: +1-859-257-2587; fax: +1-859-257-2787.
E-mail address: nbnaid2@email.uky.edu (N.B. Naidu).

0731-7085/$ – see front matter © 2004 Elsevier B.V. All rights reserved.
doi:10.1016/j.jpba.2004.01.003

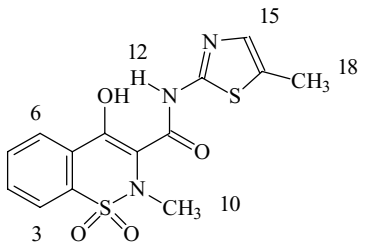

Fig. 1. Structure of meloxicam.

solutions and variations in bioavailability. Thus, increasing the aqueous solubility of meloxicam is of therapeutic importance. In this present investigation, meloxicam was complexed with cyclodextrins (α-, β- and γ-CDs) in an attempt to improve its aqueous solubility, dissolution properties.

Cyclodextrins (CDs) are cyclic (α-1,4)-linked oligosaccharides of D-glucopyranose containing a relatively hydrophobic central cavity and a hydrophilic outer surface. Cyclodextrins are able to form inclusion complexes with poorly water-soluble drugs. These inclusion complexes have been shown to improve stability, solubility, dissolution rate and bioavailability [7,8]. This improvement in hydrophilicity may be due either to the formation of inclusion complexes of a host/guest type, as a function of the structure of the oligosaccharide ring, or maybe by means of a highly homogeneous assembly between the CD and the drug in the solid state. In most cases, this association increases the solubility of poorly soluble drugs.

2. Experimental

2.1. Materials

The meloxicam sample was supplied by Sun Pharma Ltd., Mumbai, India, α-, β- and γ-CDs were obtained from Wacker Biochem Corp., USA and all other reagents and solvents were of analytical grade.

2.2. Methods

2.2.1. Preparation of solid binary systems

The following binary systems of ME and CDs were prepared at 1:1 and 1:2 molar ratios (1:1 and 1:2 M).

2.2.1.1. Physical mixtures (PM). The physical mixtures of ME and CDs in 1:1 and 1:2 M were obtained by mixing individual components that had previously been sieved (75–150 μm) together with a spatula.

2.2.1.2. Kneaded systems (KS). The physical mixtures of ME and CDs in 1:1 and 1:2 M were triturated in a mortar with a small volume of water-methanol (1:1, v/v) solution. The thick slurry was kneaded for 45 min and then dried at 45 °C until dryness. The dried mass was pulverized and sieved and a 75–150 μm granulometric sieve fraction was collected. Wetting agent (water:methanol, 1:1%, v/v) was used mainly to achieve better interaction of meloxicam with cyclodextrins during kneading process. The presence of methanol helps to improve wettability of meloxicam, there by better interaction with cyclodextrins.

2.2.1.3. Coevaporated systems (CS). The aqueous solution CD was added to a solution of meloxicam dissolved in liquid ammonia. The resulting mixture was stirred for 1 h and evaporated at a temperature of 45 °C until dry. The dried mass was pulverized and sieved and a 75–150 μm granulometric sieve fraction was collected.

2.2.2. Detection of inclusion complexation in solution state

2.2.2.1. Phase solubility studies. Excess amounts of meloxicam (50 mg) were added to 15 ml of either purified water or CD aqueous solutions (ranging in concentration from 0.003 to 0.048 M) in a series of 25 ml stoppered conical flasks. The mixtures were shaken for 48 h at room temperature (28 °C) on a rotary flask shaker. After 48 h of shaking to achieve equilibrium, 2 ml aliquots were withdrawn at 12 h intervals and filtered immediately using a 0.45 μm nylon disc filter. The filtered samples were diluted and assayed for ME by measuring absorbance at 365 nm. Shaking was continued until three consecutive estimations were the same. The solubility experiments were conducted in triplicate (coefficient of variation, CV < 2%). The blanks were performed in the same concentrations of CDs in water in order to cancel any absorbance that may be exhibited by the CD molecules. The apparent stability constants were calculated from phase solubility diagrams [9].

2.2.2.2. Mass spectrometry analysis. Electrospray ionization mass spectrometry (ESI-MS) was carried out on a Finnigan LCQ DECA iontrap mass spectrometer (San Jose, CA, USA) equipped with an electrospray ionization source. Meloxicam was dissolved in water/methanol/acetic acid (49.5:49.5:1, v/v) in the absence and presence of CDs. The final concentrations of ME and CDs were 1 and 2 mM, respectively. Infusion rates were 5 μl/min during sample analysis.

2.2.2.3. ^1H NMR spectroscopy. ^1H nuclear magnetic resonance (NMR) experiments were performed on a Varian 500 MHz Inova NMR with dual full-band channels and *z*-axis gradients using Varian *z*-axis PFG Inverse detection probe. The spectra were measured at 298 K with an operating frequency of 499.742 MHz (pw90 ^1H was 10.8 μs at tpwr of 50). Spatial connectivity between cyclodextrin and drug was established by 1D-ROE and ROESY (relaxation delay of 300 ms and a mixing time of 350 ms) experiments. The solutions of cyclodextrins, meloxicam, and solid complexes were prepared by dissolving in a 50 mM sodium borate buffer (pH 9.5), which was made up in deuterium oxide, to give a 5 mM solution. Solutions for ROESY experiments were purged under a stream of argon for 1 h prior to data collection, to reduce the amount of dissolved oxygen.

2.2.3. Detection of inclusion complexation in solid state

2.2.3.1. Differential scanning calorimetry. Thermograms of pure materials, their treated components and all binary systems were recorded on a Seiko, DSC 220C model differential scanning calorimeter (DSC, Tokyo, Japan). About 10 mg of samples were sealed in aluminum pans and heated at a heating rate of 10°C/min from 30 to 300 °C.

2.2.3.2. Powder X-ray diffractometry. The powder X-ray diffraction (XRD) patterns of pure materials, their treated counterparts and all binary systems were recorded by using an automated Philips X'Pert X-ray diffractometer (Osaka, Japan). The samples were irradiated with monochromatized Cu Kα radiation and analyzed between 2θ angles of 4 and 54°. The voltages, current and time per step used were 30 kV, 20 mA and 0.5 s, respectively.

2.2.3.3. Scanning electron microscopy. The surface morphology of pure materials, their treated counterparts and all binary systems was examined by Scanning Electron Microscope (Joel, JSM-840A, Tokyo Japan). The samples were fixed on a brass stub using double-sided tape and then gold coated in vacuum by a sputter coater. The pictures were then taken at an excitation voltage of 20 kV.

2.2.3.4. Dissolution studies. In vitro dissolution studies of pure drug and its treated samples and the prepared binary systems were carried out in 900 ml of phosphate buffer at pH 7.4 I.P. using a USP XXI type 2 Dissolution Rate Test Apparatus by the powder dispersed amount method (powder samples were spread over the dissolution medium). Samples equivalent to 15 mg of ME, a speed of 50 rpm and a temperature of 37 ± 1 °C were used in each test. A 5 ml aliquot was withdrawn at different time intervals, filtered using a 0.45 μm nylon disc filter and replaced with 5 ml of fresh dissolution medium. The filtered samples were suitably diluted, if necessary, and assayed for ME by measuring the absorbance at 365 nm. The dissolution experiments were conducted in triplicate.

3. Results and discussion

3.1. Phase solubility studies

A summary of the findings of the phase solubility studies is shown in Table 1. The phase solubility diagram was given as Fig. 2. The solubility calculated for ME in water (pH 6.2) was 12 μg/ml at 28 °C. The solubility of ME increased linearly with an increase in the concentration of CDs, giving A_L type solubility

Table 1
Summary of ME–CDs phase solubility studies

	Type of phase solubility diagram	Stability constant ± S.D. (M^{-1})	Increase of solubility (S_t/S_0)[a]
α-CD	A_L	82.12 ± 2.21	2.11
β-CD	A_L	109.97 ± 1.97	2.75
γ-CD	A_L	78.67 ± 1.93	2.05

[a] S_t, solubility of meloxicam in 15 mM of CD solutions; S_0, solubility of meloxicam in water.

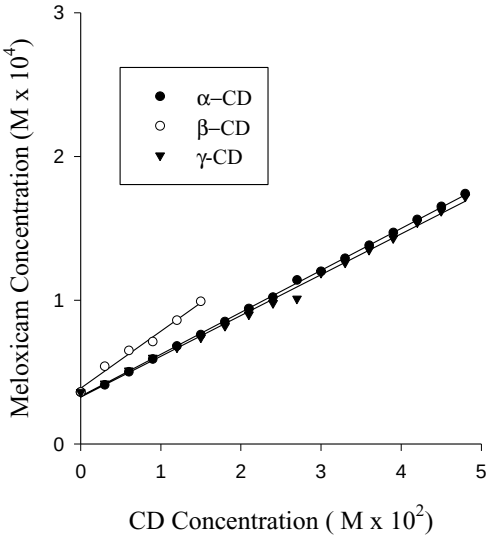

Fig. 2. Phase solubility diagram of ME–CDs solutions.

diagrams [9]. The increase in solubility in the systems is due to one or more molecular interactions between ME and CDs to form distinct species or complexes. The solubilizing efficiency of different CDs is in the order of β-CD > α-CD > γ-CD. The cavity size of the β-CD seems to be optimal for entrapment of ME molecule and consequently provides the greatest solubilization effect. The apparent stability constants ($K_{1:1}$) were calculated for these complexes from phase solubility diagrams according to the following equation:

$$K_{1:1} = \frac{\text{slope}}{S_0(1 - \text{slope})}$$

where S_0 is intercept

The stability constant values calculated were 82.12 ± 2.21, 109.97 ± 1.97 and $78.67 \pm 1.93\,M^{-1}$, respectively, for α-, β- and γ-CDs. The larger constant that was observed with β-CD indicates that ME interact more strongly with this CD.

3.2. Mass spectrometry analysis

The full scan spectrum of meloxicam showed a strong peak at $[ME]^+$ 352. The full scan spectra of the ME–CD solutions are shown in Fig. 3. The ions corresponding to the meloxicam (*m*/*z* 351.9), α-CD (*m*/*z* 972), β-CD (*m*/*z* 1135) and γ-CD (*m*/*z* 1297) were

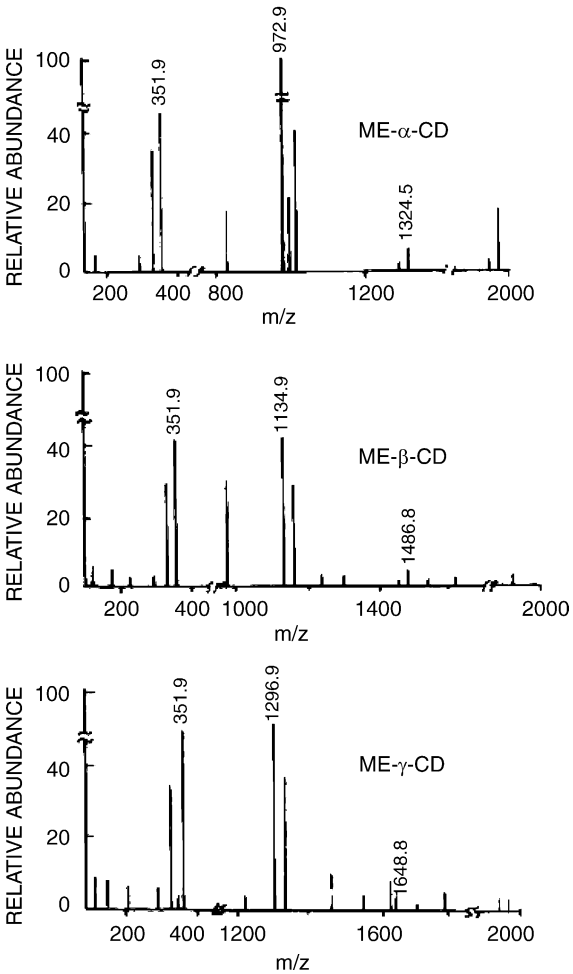

Fig. 3. ESI MS spectra of ME–CD solutions.

seen as strong peaks in the full scan spectra of the respective ME–CDs solutions. The full scan spectra of ME–CDs solutions also showed peaks at *m*/*z* 1324.5, 1486.8 and 1648.8 ions corresponding to the 1:1 M adducts of ME with α-, β- and γ-CDs, respectively. All these results suggest that ME interact with CDs forming inclusion complexes in solution state.

3.3. ^1H NMR spectroscopy

The ^1H NMR spectroscopy studies of ME with α-, β- and γ-CDs were carried out to gain insights into the complexation mode(s) of ME. The observable changes in chemical shift ($\Delta\delta$) upon complexation are

Table 2
Differences in the observed chemical shift (δ) of the cyclodextrin protons upon addition of meloxicam: (A) α-CD; (B) β-CD; (C) γ-CD

Position	CD only ^{1}H, δ (ppm)	m, J (Hz)	CD + meloxicam ^{1}H, δ (ppm)	$\Delta\delta$
(A) α-CD				
1	4.929	d, 3.5	4.910	−0.019
2	3.505	dd, 10.0, 3.0	3.488	−0.017
3	3.861	dd, 10.0., 9.0	3.824	−0.037
4	3.460	t, 9.0	3.434	−0.026
5	3.756 overlap with H-6	m	3.713	−0.043
6	3.731 overlap with H-5	m	3.795	0.064
(B) β-CD				
1	4.945	d, 3.5	4.936	−0.009
2	3.523	dd, 10.5, 3.5	3.514	−0.009
3	3.844	dd, 10.5., 9.0	3.819	−0.025
4	3.459	t, 9.0	3.454	−0.005
5	3.754 overlap with H-6	m	3.711 overlap with H-6	−0.043
6	3.754 overlap with H-5	m	3.748 overlap with H-5	−0.006
(C) γ-CD				
1	4.987	d, 3.5	4.973	−0.014
2	3.528	dd, 10.0, 3.0	3.523	−0.005
3	3.815	dd, 10.0., 9.0	3.806	−0.009
4	3.484	t, 9.0	3.458	−0.026
5	3.740 overlap with H-6	m	3.737 overlap with H-6	−0.003
6	3.740 overlap with H-5	m	3.737 overlap with H-5	−0.003

$\Delta\delta = \delta_{complex} - \delta_{free}$.

relatively modest in magnitude for all cyclodextrins. The greatest changes in chemical shift were generally observed for the upfield shifts of H-3 and H-5, which is characteristic of the formation of an inclusion complex. Unfortunately the chemical shift of the H-5 signal was not always distinguishable from the H-6 resonance. The spatial interactions between proximal protons of the cyclodextrin and guest molecule that arise through dipolar interactions were determined using one-dimensional ROE experiments (1D ROE) and ROESY experiments. In these experiments, correlations are typically observed between proximal protons that are closer than 4 Å through space. Correlation of the H-3 and H-5 protons of the cyclodextrin to the protons of the guest is strong evidence for the formation of an inclusion complex. The ^{1}H NMR data for protons of α-, β- and γ-CD's, including the complexation-induced shifts, $\Delta\delta$ ($\delta_{complex} - \delta_{free}$), in the absence and presence of ME are shown in Table 2. The ^{1}H NMR data for ME, including the complexation-induced shifts, $\Delta\delta$ ($\delta_{complex} - \delta_{free}$), in the absence and presence of α-, β- and γ-CD's are shown in Table 3. The ROESY spectras are shown in Fig. 4. In the presence of cyclodextrins almost all the

Table 3
^{1}H Chemical shift data for ME with and without CDs

Position	δ (ppm) ME	m, J (Hz)	$\Delta\delta$ (ppm) ME + α-CD	$\Delta\delta$ (ppm) ME + β-CD	$\Delta\delta$ (ppm) ME + γ-CD
3	7.735	dd, 7.5, 1.5	−0.019	−0.026	−0.025
4	7.663	td, 7.5, 1.0	−0.024	−0.021	−0.022
5	7.753	td, 7.5, 1.5	−0.024	−0.021	−0.021
6	7.953	dd,7.5, 1.0	−0.046	−0.012	−0.013
10 Me	2.770	s	−0.027	−0.021	−0.034
15	6.992	d, 1.0	0.045	−0.035	−0.015
18 Me	2.278	d, 1.0	0.014	−0.001	−0.016

$\Delta\delta = \delta_{complex} - \delta_{free}$.

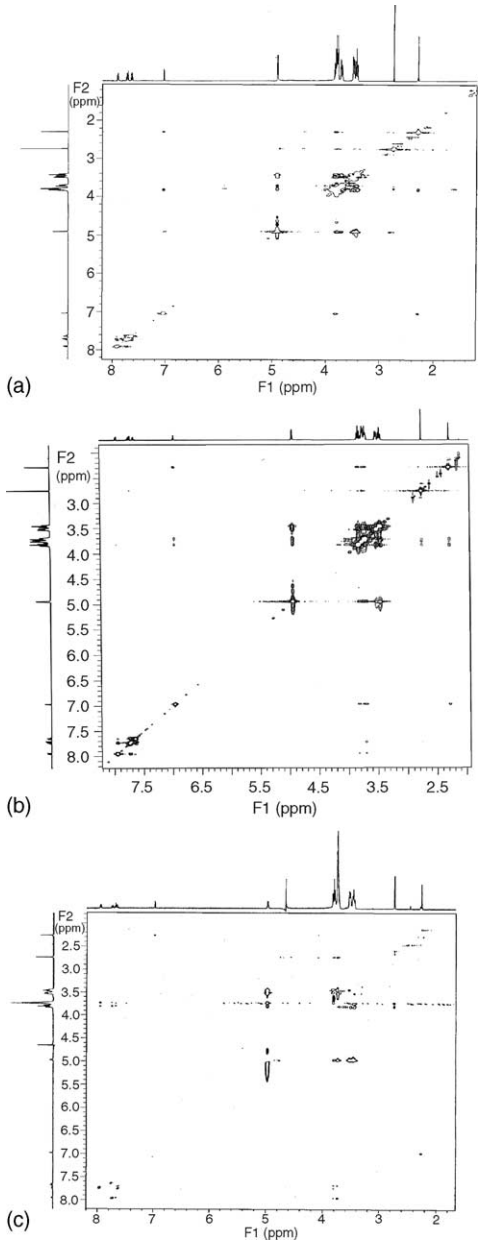

Fig. 4. ROESY spectra for (a) ME–α-CD; (b) ME–β-CD; (c) ME–γ-CD complexes.

protons in meloxicam are weakly shielded to some degree, the notable exceptions being the protons associated with the thiazole-ring (H-15 and H-18), which are deshielded in the presence of α-cyclodextrin. Strong ROE correlations (Table 4) are observed between these protons and the H-3 of α-cyclodextrin, but not the H-5, suggesting that there is shallow inclusion of the thiazole ring into the cyclodextrin cavity. In the case of ME and β-CD the H-15 and H-18 protons of meloxicam exhibit very strong spatial correlation with both the H-3 and H-5 protons of β- cyclodextrin, indicating that the thiazole ring is deeply included into the cyclodextrin cavity. However, only modest $\Delta\delta$ values are observed for the H-15 and H-18 protons of meloxicam. The disparity in $\Delta\delta$ values of these protons may be attributable to complexation-induced changes in the shielding/deshielding effects, i.e. inductive and mesomeric effects, of the substituent groups. The spatial correlation data also indicate a second mode of binding for the β-cyclodextrin complex, with the H-5 and H-6 protons of meloxicam being proximal to the H-3 and H-5 protons of the cyclodextrin. This requires the relatively non-polar ring of the benzothiazine group to be deeply included in the cyclodextrin cavity. There is no evidence for inclusion of the thiazole ring into the cavity of γ-CD. Spatial correlations are observed only between the protons of the benzothiazine group and those within the cavity of the cyclodextrin. The H-6 and H-10 protons of ME both show strong correlation to the H-5 proton of the CD. This would indicate deep binding of the drug into the cavity. Although the cavity of γ-CD is sufficiently large to accommodate the entire benzothiazine group, the possibility of the existence of multiple binding modes cannot be precluded.

3.4. Differential scanning calorimetry

The thermograms of ME and kneaded meloxicam (KME) showed a sharp endothermic peak at 257.7 °C corresponding to its melting point. However, the thermogram of CME (evaporated meloxicam) showed a broad endotherm ranging from 113.4 to 161.7 °C with a peak of 145.3 °C, which may be due to dehydration process, along with the melting endotherm at 251.8 °C. This dehydration peak may be due to the occluded water during the evaporation process which is present in the liquid ammonia. This was further confirmed from the DSC thermogram of pre-heated (0–150 °C) CME sample, where no dehydration peak was found. DSC thermograms of all CDs, i.e. α-, β- and γ-CDs, showed a broad endothermal effect ranging from 40 to 150 °C, due to their dehydration process. The thermal curves of the binary systems of ME with α- and β-CDs

Table 4
Summary of ROE intermolecular interactions (very strong*/strong/weak)

Position	^{1}H, δ (ppm)	m, J (Hz)	α-CD	β-CD	γ-CD
3	7.735	dd, 7.5, 1.5	–	–	H-3, H-5
4	7.663	td, 7.5, 1.0	–	H-5	H-3, H-5
5	7.753	td, 7.5, 1.5	–	H-3, H-5	H-3
6	7.953	dd, 7.5, 1.0	–	H-3, H-5	H-3, H-5
10 Me	2.770	s	H-3	H-3, H-5	H-3, H-5
15	6.992	d, 1.0	H-3	H-3*, H-5*	–
18 Me	2.278	d, 1.0	H-3	H-3*, H-5*	–

invariably showed the typical meloxicam endotherm, which progressively reduced in its peak intensity and shifted to lower temperatures passing from physical mixtures to kneaded and coevaporated systems. This marked reduction in intensity and/or broadening and shift to a lower temperature of the ME endotherm in kneaded and coevaporated systems indicates a partial inclusion of ME in the CD cavities. In the case of the ME–γ-CD binary systems, the characteristic thermal profile of ME was invariably present in the physical mixtures of both ratios i.e. 1:1 and 1:2 M. On the contrary, in the binary systems prepared by the kneading and coevaporation methods showed the complete disappearance of the ME endothermic peak indicating the formation of an amorphous solid dispersion, the molecular encapsulation of the drug inside the CD cavity, i.e. a true inclusion complex (Fig. 5).

3.5. XRD studies

Power X-ray diffractometry is a useful method for the detection of cyclodextrin complexation in powder or microcrystalline states. The diffraction pattern of the complex should be clearly distinct from that of the superimposition of each of the components if a true inclusion complex has been formed. Crystallinity was determined by comparing some representative peak heights in the diffraction patterns of the binary systems with those of a reference. The relationship used for the calculation of crystallinity was relative degree of crystallinity (RDC) $= I_{sam}/I_{ref}$, where I_{sam} is the peak height of the sample under investigation and I_{ref} is the peak height at the same angle for the reference with the highest intensity [10]. Pure drug peak at 25.7° (2θ) was used for calculating RDC of kneaded and coevaporated binary systems. The RDC values of corresponding binary systems are given in Table 5. A similar diffraction pattern with several intense peaks was achieved for any sample of ME, independently of the previous treatment, conclusively displaying its crystalline structure. However, the CME showed a diffraction

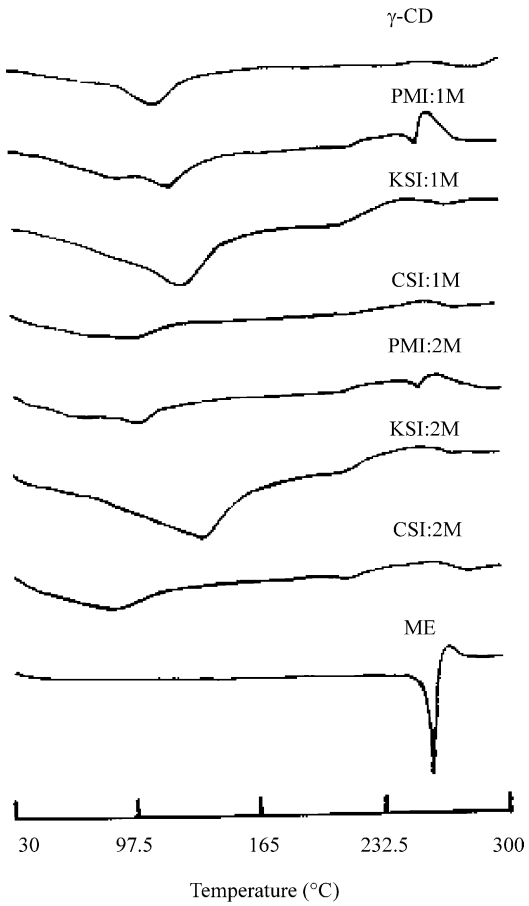

Fig. 5. DSC thermograms of ME and ME–γ-CD binary systems.

Table 5
RDC values of ME–CD binary systems

Sample	RDC			
	KS 1:1 M	CS 1:1 M	KS 1:2 M	CS 1:2 M
ME–α-CD	0.375	0.270	0.152	0.047
ME–β-CD	0.418	0.374	0.189	0.079
ME–γ-CD	–	–	–	–

pattern similar to that of pure ME but with relatively less intense peaks. In the case of α- and γ-CD samples a similar diffraction pattern was observed irrespective of method of treatment. In the case of the β-CD samples kneaded β-CD showed a diffraction pattern similar to that of pure β-CD, but with a reduction in peak intensities. The evaporated β-CD showed a diffraction pattern similar to that of pure β-CD but with a relatively more intense peaks. The X-ray diffraction patterns of ME–α-CD and ME–β-CD 1:1 and 1:2 M binary systems showed all the principle peaks of ME, α-CD and β-CD. However, the peak intensities of the 1:2 M binary systems are lower than the corresponding 1:1 M binary systems. The diffraction patterns are the sum of each component, indicating the presence of ME in a crystalline state. These results suggest that no alteration was produced in the crystal structure of ME, but that the crystallinity was modified, since the peak position (angle of diffraction) is an indication of crystal structure and the peak heights in a diffractogram are a measure of the sample crystallinity. From the RDC values (Table 5) it is seen that when pure ME was considered as reference sample, a decrement in crystallinity was observed in all of the ME–α-CD and ME–β-CD 1:1 and 1:2 M binary systems and is in the in the order of CS > KS. These observations were in accordance with the results of the DSC studies, indicating that there was no true inclusion complexation between ME and either α-CD, or β-CDs in solid state at both the molar ratios. In the case of the diffraction patterns obtained with the ME–γ-CD 1:1 and 1:2 M physical mixtures (Fig. 6), all the principal peaks of ME and γ-CD were observed. Overlap of the drug peaks by the γ-CD peaks was also observed. The diffractograms of ME–γ-CD 1:1 and 1:2 M KS and the CS binary systems differed from those of the corresponding physical mixtures, where the characteristic peaks of ME, particularly at 25.7° (2θ), disappeared,

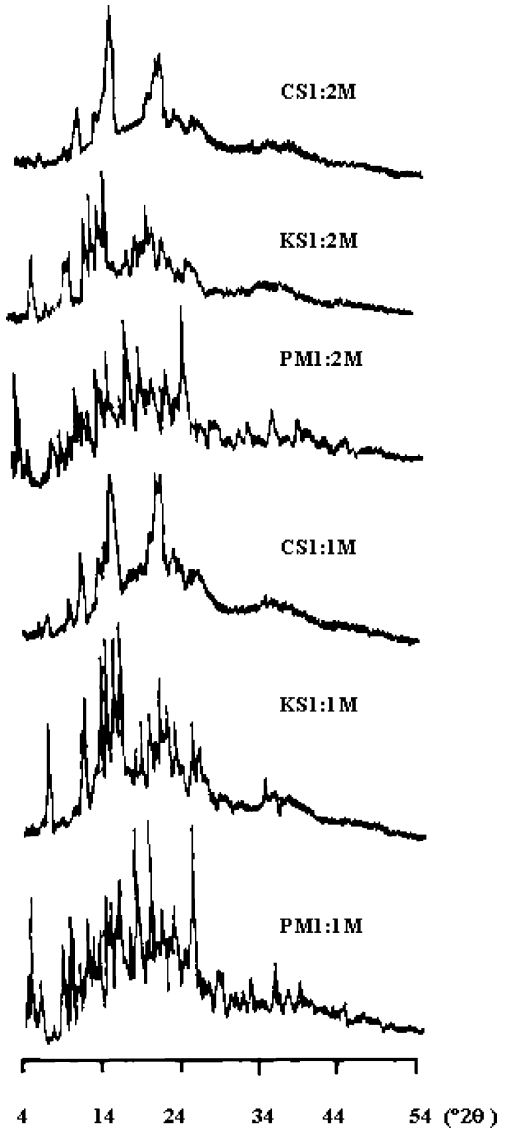

Fig. 6. Powder X-ray diffractograms of ME–γ-CD binary systems.

indicating the formation of inclusion complex in these systems. These observations were in accordance with the results of the DSC studies. In the case of the diffraction patterns of all the ME–CD 1:2 M physical mixtures, all the principal peaks of ME and CDs are present, although with a lower intensity than with the ME–CD 1:1 M physical mixtures. This difference in peak intensities in different physical mixtures is due to the presence of different amounts of drug and

cyclodextrin. Due to the presence of higher amounts of ME in the 1:1 M physical mixtures compared with the 1:2 M counterparts, the intensity of the ME peaks were higher in the 1:1 M physical mixtures. The decline in the crystallinity of the physical mixtures (as evidenced by peak heights) compared with pure ME was due to their composition since this was a pure substance being compared to a physical mixture of two substances with different diffraction patterns.

3.6. Scanning electron microscopy

Scanning electron microscopy (SEM) is used to study the microscopic aspects of the raw materials i.e. CDs and drug substances and the products obtained by different methods of preparation like kneading and coevaporation etc. Even if there is a clear difference in crystallization state of the raw materials and the products, this study is inadequate to affirm inclusion complexation, but nevertheless helps to assess the existence of a single component in the preparations obtained. The commercial ME particles are in the form of prismatic crystals with a relatively well-defined outline. The smaller particles are adhered to surfaces of larger ones. The kneaded sample (KME) displayed similar appearance as the commercial sample with out changing the shape and size of the particles. Where as the evaporated particles were well-developed rectangular crystals, where smaller particles are adhered to surfaces of larger ones (Fig. 5). The commercial α-CD particles were prismatic with well-developed faces. The kneaded and evaporated particles were irregular in shape. All the β-CD particles, i.e. pure β-CD, kneaded (K β-CD) and evaporated (C β-CD),

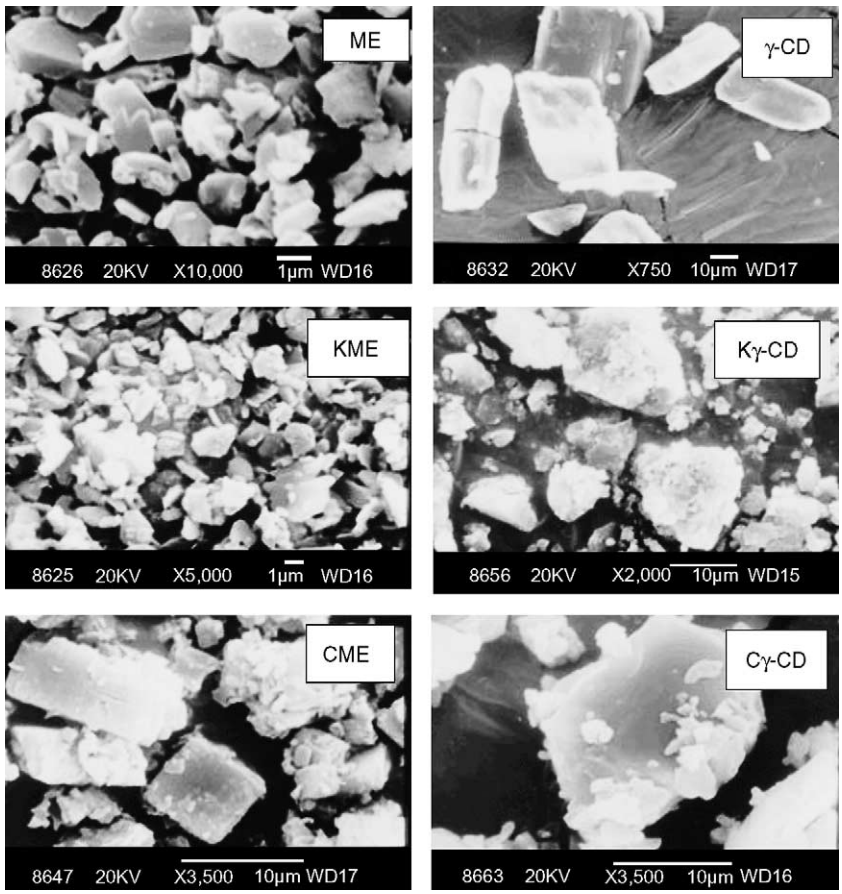

Fig. 7. SEM photographs of ME, γ-CD and their corresponding treated samples.

were irregular in shape. The micrographs of commercial β-CD showed the adherence of smaller particles on to the surfaces of larger particles. The commercial γ-CD particles were tabular in shape with slightly diffused outlines, whereas the kneaded and evaporated particles were irregular in shape (Fig. 7). All of the commercial CDs (α-, β-, γ-CD) showed crack on the surfaces. All the physical mixtures (ME–α-CD, ME–β-CD and ME–γ-CD) were characterized by the presence of particles of both the components i.e. ME and CDs without any modification in shape or size. In contrast all the scanning electron micrographs of kneaded and coevaporated systems of ME–CDs reveals the effect of kneading and coevaporation techniques, where the samples were homogeneous, and it is impossible to differentiate crystals of both components indicating the better interaction of drug particles with CDs. The particles were all irregular in shape, except in ME–γ-CD coevaporated systems. In the case of ME–γ-CD coevaporated systems the particles are rectangular in shape (Fig. 8). Although SEM technique is inadequate to conclude in genuine complex formation, the obtained micrographs support the idea of the consecution of a new single component. Thus, in the case of ME–γ-CD 1:2 M kneaded and coevaporated binary systems, along with the results of DSC and XRD studies one can confirm the inclusion complexation.

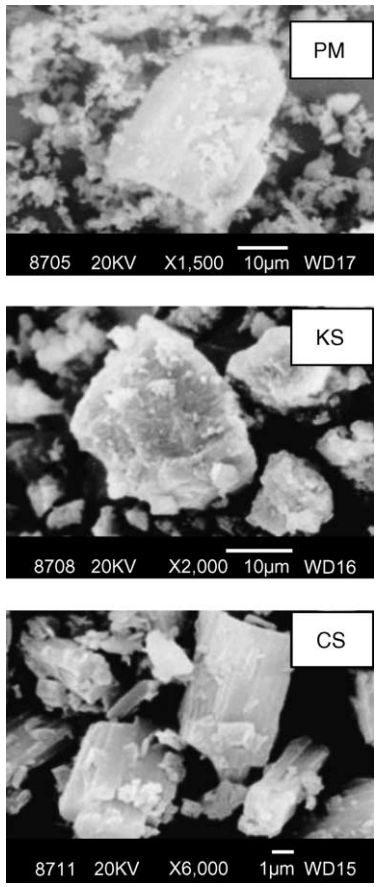

Fig. 8. SEM photographs of ME–γ-CD 1:2 M binary systems.

3.7. Dissolution studies

When an assumed drug–CD binary system is dispersed in a dissolution medium, a very rapid dissolution is often observed. Dissolution rate tests are based on this observation in order to characterize the inclusion complexation between drug and cyclodextrin. The most often used dissolution rate tests are the rotating disk method and dispersed amount method. In the present investigation, dispersed amount method is used to investigate the various dissolution parameters of ME and ME–CD binary systems. The results in terms of dissolution efficiency [11] at 10 min (DE_{10}, %) and percent of active ingredient dissolved at 30 min (DP_{30}) are presented in Table 6. DE is defined as the area under the dissolution curve up to the time, t expressed as a percentage of the area of the rectangle described by 100% dissolution in the same time.

$$\text{Dissolution efficiency (DE)} = \left(\frac{\int_0^t y\,\mathrm{d}t}{y_{100}t}\right)100$$

The dissolution efficiency can have a range of values depending on the time interval chosen. In any case, constant time intervals should be chosen for comparison. In the present investigation DE_{10} values were calculated from the dissolution data of each product and used for comparison. One-way ANOVA was used to test the statistical significance of differences between pure and treated samples. Significance of differences in the means was tested using Fishers LSD at 95% confidence. The DP_{30} and DE_{10} values of CME are significantly higher ($P < 0.05$) when compared to pure ME and KME. The increase in dissolution rate and efficiency values that were recorded for the physical mixtures may be explained on the basis of the solubility of

Table 6
Mean ± S.D. values of DP_{30} and DE_{10} for ME and ME–CD binary systems ($n = 3$)

Sample	DP_{30}	DE_{10} (%)
ME	9.18 ± 0.14	1.60 ± 0.14
KME	12.46 ± 0.03	2.90 ± 0.22
CME	60.30 ± 1.32	18.14 ± 0.33
ME–α-CD PM 1:1 M	36.40 ± 1.02	7.98 ± 0.10
ME–α-CD KS 1:1 M	98.52 ± 1.21	56.80 ± 0.88
ME–α-CD CS 1:1 M	99.99 ± 0.01	63.48 ± 0.29
ME–α-CD PM 1:2 M	50.68 ± 0.48	8.88 ± 0.34
ME–α-CD KS 1:2 M	100.00 ± 0.02	66.77 ± 0.15
ME–α-CD CS 1:2 M	100.24 ± 0.40	71.91 ± 0.30
ME–β-CD PM 1:1 M	31.31 ± 0.42	4.96 ± 0.30
ME–β-CD KS 1:1 M	68.35 ± 0.96	20.96 ± 0.39
ME–β-CD CS 1:1 M	81.26 ± 0.93	30.64 ± 1.56
ME–β-CD PM 1:2 M	33.87 ± 0.48	7.83 ± 0.06
ME–β-CD KS 1:2 M	99.76 ± 0.34	64.49 ± 0.49
ME–β-CD CS 1:2 M	100.03 ± 0.05	68.64 ± 0.38
ME–γ-CD PM 1:1 M	40.33 ± 0.34	10.07 ± 0.08
ME–γ-CD KS 1:1 M	100.00 ± 0.02	65.59 ± 0.14
ME–γ-CD CS 1:1 M	100.01 ± 0.01	69.91 ± 0.32
ME–γ-CD PM 1:2 M	63.56 ± 0.48	16.59 ± 0.29
ME–γ-CD KS 1:2 M	100.01 ± 0.01	71.83 ± 0.20
ME–γ-CD CS 1:2 M	100.27 ± 0.14	73.88 ± 0.18

the drug in aqueous CDs solutions. Since the CDs dissolve more rapidly in the dissolution medium than the pure drug, it can be assumed that, in the early stages of the dissolution process, the CD molecules will operate locally on the hydrodynamic layer surrounding the particles of the drug, this action resulting in an in situ inclusion process, which produces a rapid increase of the amount of the dissolved drug [12]. The DE_{10} and DP_{30} values of the binary systems that were prepared by the kneading and the coevaporation methods were relatively high when compared with the values from the physical mixtures and ME alone. Overall, the rank order of improvement in dissolution properties of ME with different CDs is γ-CD > α-CD > β-CD. The DE_{10} and DP_{30} values of the ME–CDs coevaporated systems were higher than those of the kneaded systems. This may be due to the less crystallinity of the ME–CDs coevaporated systems than that of the kneaded systems (other products) as indicated by the RDC values (Table 5) from the X-ray diffractograms. The differences observed between the solubilizing efficiency and stability constant values did not reflect the similar differences in improving the dissolution rate and efficiency values of the binary systems. Various authors suggested that dissolution rates from drug–CD binary systems are also dependent on other factors, such as diffusion and dissociation of the complex in the dissolution medium [13,14] or decrease in crystallinity and enhanced wettability of the drugs by the inclusion complexation [15]. The higher dissolution rate and efficiency values observed with the ME–γ-CD 1:1 and 1:2 M kneaded and coevaporated binary systems when compared with other ME–CD 1:1 and 1:2 M kneaded and coevaporated binary systems may be due to the formation of amorphous solid inclusion complexes as indicated from the DSC and XRD diffractograms.

4. Conclusions

Physicochemical characterisation of ME–CD binary systems in solution state by phase solubility, mass spectrometry and ^{1}H NMR studies revealed 1:1 M complexation of meloxicam with all CDs. A true inclusion of ME with γ-CD at 1:1 and 1:2 M kneaded and coevaporated binary systems in solid state was confirmed by DSC, powder XRD studies. Dissolution properties of ME–CDs binary systems were superior when compared to pure ME. Overall coevaporated systems showed superior dissolution properties when compared to kneaded systems and physical mixtures. Thus, the pharmaceutical properties like aqueous solubility and dissolution rate of ME can be improved by complexation with cyclodextrins.

References

[1] G. Engelhardt, D. Homma, K. Schlegel, C. Schnitzeler, R. Utzmann, Inflamm. Res. 44 (1995) 423–433.
[2] G. Engelhardt, R. Bogel, C. Schnitzeler, R. Utzmann, Biochem. Pharmacol. 51 (1996) 21–28.
[3] L. Churchill, A.G. Graham, C.K. Shih, D. Pauletti, P.R. Farina, P.M. Grob, Inflamm. Pharmacol. 4 (1996) 125–135.
[4] M. Pairet, G. Engelhardt, in: J. Vane, J. Botting, R. Botting (Eds.), Improved Nonsteroidal Anti Inflammatory Drugs—COX-2 Enzyme Inhibitors, Kluwer Academic Publishers, Dordrecht, 1996, pp. 103–119.
[5] M. Distel, C. Mueller, E. Bluhmki, Inflamm. Pharmacol. 4 (1996) 71–81.
[6] D. Truck, U. Busch, G. Heinzel, H. Narjes, Drug Res. 47 (1997) 253–258.
[7] D. Duchene, D. Wouessidjewe, Drug Dev. Ind. Pharm. 16 (1990) 2487–2499.

[8] O. Bekers, E.V. Uijtendal, J.H. Beijnen, A. Bult, W.J. Underberg, Drug Dev. Ind. Pharm. 17 (1991) 1503–1549.
[9] T. Higuchi, K.A. Connors, in: C.N. Reilly (Ed.), Advances in Analytical Chemistry Instrumentation, Interscience, New York, vol. 4, 1965, pp. 117–212.
[10] J.A. Ryan, J. Pharm. Sci. 75 (1986) 805–807.
[11] K.A. Khan, J. Pharm. Pharmacol. 27 (1975) 48–49.
[12] O.I. Corrigan, T. Stanley, J. Pharm. Pharmacol. 34 (1982) 621–626.
[13] M. Donbrow, E. Touitou, J. Pharm. Sci. 67 (1978) 95–98.
[14] K. Uekama, S. Narisawa, F. Hirayama, M. Otagiri, Int. J. Pharm. 16 (1983) 327–338.
[15] R. Gandhi, A.H. Karara, Drug Dev. Ind. Pharm. 14 (1988) 657–682.